

Adsorption of furfural from torrefaction condensate using torrefied biomass

Doddapaneni, T. R. K.; Jain, R.; Praveenkumar, R.; Rintala, J.; Romar, H.; Konttinen, J.;

Originally published:

October 2017

Chemical Engineering Journal 334(2018), 558-568

DOI: <https://doi.org/10.1016/j.cej.2017.10.053>

Perma-Link to Publication Repository of HZDR:

<https://www.hzdr.de/publications/Publ-25861>

Release of the secondary publication
on the basis of the German Copyright Law § 38 Section 4.

CC BY-NC-ND

Adsorption of furfural from torrefaction condensate using torrefied biomass

Tharaka Rama Krishna C Doddapaneni ^{a*}, Rohan Jain^{a, b}, Ramasamy Praveenkumar^a, Jukka Rintala^a, Henrik Romar^c, Jukka Konttinen^a

^a Department of Chemistry and Bioengineering, Tampere University of Technology, P.O. Box 541, FI-33101 Tampere, Finland

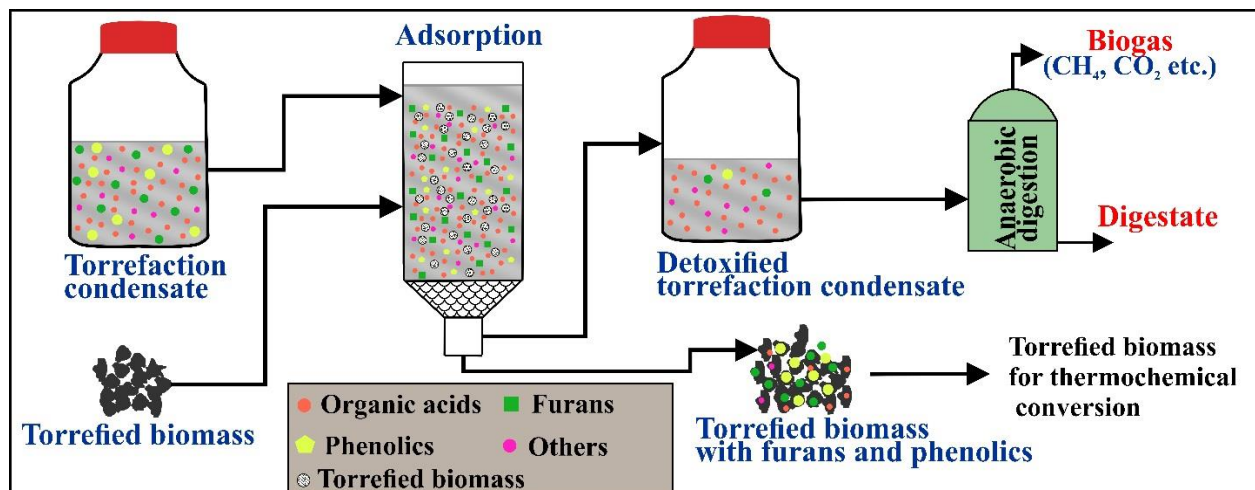
^b Helmholtz Institute Freiberg for Resource Technology, Helmholtz-Zentrum Dresden-Rossendorf, Bautzner Landstrasse 400, 01328 Dresden, Germany

^c University of Oulu, Research Unit of Sustainable Chemistry, P.O.Box 3000, FI-90014 University of Oulu, Finland

*Corresponding author:

E-mail: tharaka.doddapaneni@tut.fi ; Tel: +358 – 402137933 (T.R.K.C. Doddapaneni)

26 **Graphical abstract**



27
28
29
30
31
32
33
34
35
36
37
38
39

40 **Abstract:**

41 Torrefaction is a biomass energy densification process that generates a major byproduct in the form
42 of torrefaction condensate. Microbial conversion of TC could be an attractive option for energy
43 integration within torrefaction process. However, TC contains several compounds, such as furfural,
44 5-hydroxymethylfurfural and guaiacol that are inhibitory to microbes. In this study, for the first time,
45 we reported detoxification of TC, by removing the major inhibitory compound furfural, using
46 torrefied biomass (TB) and later used the detoxified TC for anaerobic digestion. The effect of varying
47 TB production temperature (225–300 °C), TB dosage (25–250 g/L), initial pH (2–9), and contact time
48 (1–12 h) on furfural adsorption was studied with batch adsorption experiments. Mechanism of
49 furfural adsorption on torrefied biomass was best represented by pseudo second order kinetic model.
50 The adsorption of furfural and other inhibitory compounds on TB was likely a hydrophobic
51 interaction. A maximum of 60% of furfural was adsorbed from TC containing 9000 mg furfural/L
52 using 250 g/L of TB in batch adsorption. For, column (20 mm internal diameter and 200 mm bed
53 height), the saturation time for furfural adsorption was around 50 min. Anaerobic digestion of the
54 detoxified TC shows that the lag phase in methane production was reduced from 25 d to 15 d for 0.2
55 $V_{\text{substrate}}:V_{\text{inoculum}}$ loading. The study shows that TC can be effectively detoxified using TB for
56 microbial conversion and can efficiently be integrated within the torrefied biomass pellet production
57 process.

58

59

60

61

62 **Key words:** Detoxification; Anaerobic digestion; pellets; torrefaction volatiles; Energy

63 densification

64 **1. Introduction**

65 Torrefaction is a pretreatment method for biomass upgradation, where the biomass is heated
66 slowly at a temperature range of 200-300 °C in an inert environment in order to increase the energy
67 density and hydrophobicity by lowering the moisture content of the biomass [1]. In the recent days
68 the research interest on torrefaction process is increasing owing to high commercial demand of
69 torrefied biomass, projected to be 70 million tons per year by 2020 globally [2].

70 The two major technical challenges in commercialization of torrefaction technology are
71 handling the volatile gases that are produced during the torrefaction and the energy integration within
72 the process [1]. At present, the volatile gases produced are combusted back to meet the energy
73 requirements for biomass drying and torrefaction. However, owing to their high water and CO₂
74 content, the torrefaction volatiles have low heating value. In addition, presence of different types of
75 organic acids makes them very corrosive to the combusting equipment [1,3] Hence, advanced process
76 integration approaches are required for better utilization of torrefaction volatiles and thereby
77 improving the overall efficiency and economic viability of the torrefaction system [3,4]

78 The torrefaction condensate (obtained by condensing the volatiles) mainly contains water and
79 acetic acid. Recently, Doddapaneni et al. (2017) [4] reported that torrefaction condensate, with ~50
80 g/L of acetic acid, can be used as substrate for anaerobic digestion (AD) for bio-methane production.
81 However, owing to the presence of inhibitory compounds such as furfural, 5-Hydroxymethylfurfural
82 (5-HMF) and guaiacol, the methane production was inhibited at higher substrate loading [3]. In order
83 to improve the methane production, concentration of these inhibitory compounds should be
84 significantly decreased in the torrefaction condensate.

85 Adsorption is a cost-effective method for removal of inhibitory compounds from the pyrolysis
86 oil and biomass hydrolysate [5,6]. Polymeric adsorbents such as XAD-4 and XAD-7 was shown to
87 adsorb 90 and 80 mg of furfural per g of adsorbent from corn fiber hydrolysate [5]. Other study [7]
88 reported that the adsorption of phenol and furfural from oat hull hydrolysate using powdered activated

89 carbon improved the bioproduction of xylitol by 10%. However, due to the large concentration of
90 furfural (XX g/L) in the torrefaction condensate, a cheap and readily available adsorbent with
91 reasonable adsorption capacity is required. Torrefied biomass could be an alternative adsorbent due
92 to their hydrophobic nature as furfural is also hydrophobic, cost-effectiveness and easy availability
93 (REF). However, there are no studies on the removal of inhibitory compounds from torrefaction
94 condensate using torrefied biomass and the further application of detoxified torrefaction condensate
95 for bioconversion.

96 Torrefaction process reduces the energy required for biomass grinding but subsequently, it
97 increases the energy requirement for pelletization owing to the increase in the biomass brittleness [8].
98 The energy required to pelletize the raw biomass and torrefied biomass are in the range of 757 kJ/kg
99 and 1164 kJ/kg respectively [9]. Preconditioning of torrefied biomass with water to a moisture content
100 of 10% [10] or addition of binding materials, such as wheat flour [9], lignin, starch, calcium hydroxide
101 and sodium hydroxide [11,12] has been reported to improve the properties of the pellets. However,
102 this external addition of binders would add to the production cost and also sourcing binders for large
103 production volumes would be challenging [13].

104 Figure 1 illustrates an integrated process to address the above-discussed issues i.e. (i)
105 microbial inhibition with torrefaction condensate: through torrefied biomass based adsorption of
106 inhibitory compounds, and (ii) the supply of binders for torrefied biomass pelletization: through
107 adsorbed compounds from torrefaction condensate. The proposed approach is to use a part of torrefied
108 biomass as an adsorbent for removal of the inhibitory compounds from the condensate. Following
109 adsorption, the water content and compounds adsorbed on the biomass will themselves add binding
110 effects and thereby could reduce the energy requirement in pelletization [14]. Moreover, the torrefied
111 biomass with compounds adsorbed to them could be mixed with rest of the torrefied biomass before
112 pelletizing, which will improve the quality and durability of the pellets. The torrefaction condensate
113 after adsorption (detoxified condensate) can be used in AD process.

114

115

<Figure 1>

116

117

118

119

120

121

122

123

124

125

126

127

128

129

2. Materials and methods

130

2.1 Torrefaction process

131

132

133

134

135

136

137

Torrefied biomass and torrefaction condensate were produced as described by Doddapaneni et al. [4]. Briefly, Finnish pine wood chips were air dried at 105 °C for 24 h in an electrically heated oven. The reactor (Fig. S1) temperature was raised from room temperature (20 °C) to a final torrefaction temperature i.e. 225, 275 or 300 °C and maintained at that temperature for 2 h. The fluctuation in the reactor temperature was maintained within ± 5 °C during the isothermal period by circulating water through the coils wrapped around the reactor. In each run, one kg of biomass was loaded into the reactor. The volatiles released during the torrefaction process were condensed using

138 water circulated condenser and a glass bottle submerged in an ice bath. The condensate was stored at
139 4 °C to prevent further aging reactions. The torrefaction condensate has a tendency to form settled tar
140 that is viscous and sticky in nature. This viscous tar (~ 5 vol. %) was removed by simple decantation
141 and the torrefied biomass was grinded using Restsch ZM200 centrifugal mill prior to the adsorption
142 experiments. The grinded biomass was sieved to a particle size of <100 µm.

143

144 *2.2 Characterization of torrefied biomass*

145 Torrefied biomass was characterized using scanning electron microscopy (SEM) and
146 Brunauer–Emmett–Teller (BET) analysis. Pore size distribution and surface area measurements were
147 evaluated according to Baret-Yoymer-Halenda (BJH) and BET model, respectively.

148

149 *2.3. Batch adsorption experiments*

150 All the batch adsorption experiments were carried out in a total volume of 20 mL, with
151 continuous mixing at 150 rpm and 20 °C. The kinetics of furfural adsorption using torrefied biomass
152 was studied for 12 h at an initial furfural concentration of 6000 mg/L and pH 3.6, and torrefied
153 biomass concentration varying from 25 - 150 g/L. All the subsequent batch adsorption experiments
154 were carried out for the duration of 12 h as the equilibrium was achieved. For the isotherm study, the
155 initial furfural concentration was varied from 300 - 6000 mg/L with pH of 3.6 and torrefied biomass
156 concentration of 50 g/L. The effect of pH on furfural adsorption was studied by varying the initial
157 furfural solution pH from 2 to 9, with initial furfural concentration of 6000 mg/L and torrefied
158 biomass concentration of 100 g/L. The effect of biomass dosage on furfural adsorption was studied
159 by varying torrefied biomass concentration from 25 - 150 g/L, with initial furfural concentration of
160 6000 mg/L and pH of 3.6. In case of batch adsorption studies with torrefaction condensate, the
161 torrefied biomass dosage of 25, 50, 100, 200 and 250 g/L was added to 10 mL of torrefaction

162 condensate. Torrefaction condensate was used at its original pH in all adsorption tests carried out in
163 this study. The solid-liquid separation was achieved by centrifuging the samples at 5018 xg for 5 min.
164 Supernatants were filtered using 0.45 μm (Chromafill® - PET 45/25) prior to gas chromatography
165 mass spectrometer (GC-MS) analysis. All the batch adsorption experiments were carried out in
166 duplicates and if the difference was more than 10%, the experiments were repeated.

167

168 *2.4. Column adsorption experiments*

169 The column experiments were carried out in glass column of internal diameter of 10 and 20
170 mm and the length of 300 mm. Borosilicate glass beads (2 mm dia) were used to pack torrefied biomass
171 from top and bottom in the column. This glass bead packing (2 cm height) was also helpful in allowing
172 uniform distribution of the adsorbate in the column by preventing backlash. The effective bed height
173 of adsorbent (i.e. torrefied biomass) was 200 mm. The amount of torrefied biomass filled in 10 and
174 20 mm columns were 7 g and 20 g, respectively. Either the standard furfural solution with 6000 mg/L
175 with initial pH of 3.6 or the torrefaction condensate were loaded into column using peristaltic pump
176 at 1 mL/min. Aliquots from the column were collected every 5 min for GC-MS analysis. Control
177 experiments with borosilicate glass beads were carried out to rule out adsorption of furfural on them.

178

179 *2.5. Anaerobic digestion (AD) batch assay*

180 The AD batch assays of torrefaction condensate before and after detoxification was studied,
181 using 120 mL serum bottles at mesophilic condition i.e. 35 °C for 35 d. The operating volume was
182 60 mL. The substrate to inoculum ratio ($VS_{\text{substrate}}:VS_{\text{inoculum}}$) of 0.1 (non-inhibitory concentration)
183 and 0.2 (inhibitory concentration) were tested. Granular sludge collected from the mesophilic upflow
184 anaerobic sludge blanket (USAB) reactor that treats waste water from an integrated beta-amylase and

185 ethanol plant (Jokioinen, Finland) was used as inoculum for AD batch assays. Detailed methodology
186 has been previously reported [4].

187

188 *2.6 Analytical methods*

189 Surface characteristics of torrefied biomass was analyzed using scanning electron microscopy
190 JSM –T10 (Jeol, USA). Specific surface area (SSA) and pore size distributions were measured using
191 a Micrometrics ASAP 2020 (Norcross, USA) by physical adsorption of nitrogen. For adsorption tests,
192 about 100 mg of sample was loaded into a quartz tube. Prior to adsorption tests, contaminating gases
193 from samples were removed using 10 μm Hg at a temperature of 150 $^{\circ}\text{C}$. Detailed methodology has
194 been reported by Kramb et al. (2017) [15].

195 Gas chromatograph (GC; Agilent series 6890) equipped with mass spectrometry (MS)
196 detector (Agilent 5975B) and the capillary column HP-5MS (30 m, 0.25 mm ID, 0.25 μm film
197 thickness; Agilent) was used to analyze both standard furfural solution and torrefaction condensate
198 before and after adsorption experiments. In case of standard furfural solution, initially the GC column
199 was held for 2 min at 50 $^{\circ}\text{C}$, and followed by a ramp of 5 $^{\circ}\text{C}/\text{min}$ to a temperature of 250 $^{\circ}\text{C}$. Later,
200 the oven was heated to a final temperature of 280 $^{\circ}\text{C}$ at 10 $^{\circ}\text{C}/\text{min}$ and held for 10 min. The helium
201 gas with a flow rate of 1 mL/min was used as a carrier gas. The injection temperature was 250 $^{\circ}\text{C}$.
202 The injection volume was 0.2 μL with a split ratio of 20:1. In case of torrefaction condensate analysis,
203 the oven temperature was raised at a heating rate of 2 $^{\circ}\text{C}/\text{min}$ to a temperature of 180 $^{\circ}\text{C}$ and then to
204 a final temperature of 280 $^{\circ}\text{C}$ at 10 $^{\circ}\text{C}/\text{min}$. The oven was held at final temperature for 5 min. The
205 MS temperature was maintained at 250 $^{\circ}\text{C}$.

206 The total solids (TS) and volatile solids (VS) of the inoculum and the torrefaction condensate
207 was tested as described by Doddapaneni et al. [4]. The methane production was tested using GC
208 following the procedure described in our earlier study [4].

209 **3. Results**

210 *3.1 Characterization of the adsorbent (torrefied biomass)*

211 Figure 2 shows SEM images of the pine wood biomass torrefied at 225, 275 and 300 °C. It
212 can be observed that the porosity of biomass is increasing with increasing torrefaction temperature.
213 At temperature 225 °C, no specific surface area (SSA) and pore diameter was detected by the BET
214 analysis (Table 1). The further increase in temperature to 275 °C led to increase in SSA. However,
215 SSA decreased with further raise in temperature to 300 °C.

216 <Figure 2>

217 *3.2 Characterization of torrefaction condensate*

218 Torrefaction condensate mainly contains water, organic acids, aldehydes and phenolic
219 compounds. The pH of torrefaction condensate was around 2.1. The concentration of acetic acid,
220 furfural were, 80 and 9 g/L, respectively for the torrefaction condensate produced at 300 °C. The VS
221 was around 11%.

222

223 *3.3 Influence of torrefaction temperature on furfural adsorption*

224 The influence of torrefaction temperature to produce torrefied biomass on furfural adsorption
225 was studied (Figure S2 in supplementary Information) . Furfural adsorption (%) increased from 47%
226 at 225 °C to 77% at 300 °C with 150 g torrefied biomass/L. Because of the higher adsorption, the
227 torrefied biomass produced at 300 °C was used in all our adsorption experiments.

228

229 *3.4 Batch adsorption of furfural*

230 *3.4.1 Kinetic study*

231 The influence of contact time was studied by varying the reaction duration from 1 to 12 h
 232 (Fig. 3a). The adsorption of furfural was relatively fast and more than 85% of maximum q_e (mg of
 233 furfural adsorbed per g of torrefied biomass) was achieved in first 2 h. The kinetic analysis of the
 234 adsorption of furfural on torrefied biomass was made using pseudo first order and second order kinetic
 235 models (Add references for these equations – May be a review paper) (more details in supplementary
 236 information).

237 <Figure 3>

238 The plot of $\log (q_e - q_t)$ versus t , the plot of q_t/t versus t represents the first order and second
 239 order kinetic models respectively. The rate constants (k_f), and (k_s), for first and second order kinetic
 240 models, respectively were presented in Table 2. From Fig. 3b and Table 2 it can be observed that the
 241 pseudo second order model fits well with the R^2 values greater than 0.99. The variation between the
 242 calculated $q_{e \text{ cal.}}$ and the experimental q_e values were varying between 17 - 51% and 6 - 8% for pseudo
 243 first order and second order kinetic models, respectively further suggesting better fit for pseudo
 244 second order kinetic model.

245 <Table 2>

246 The rate constant of pseudo second order kinetic model is a combination of external mass
 247 transfer, film diffusion and intra-particle diffusion. Thus, the adsorption of furfural on to torrefied
 248 biomass was further studied to identify the rate limiting step in the process. The external mass transfer
 249 model, furfural transfer across the boundary layer (Boyd's film diffusion model), intra-particle
 250 diffusion (Webber-Morris) and pore diffusion model (Bangham's model) were tested.

251 The mass transfer of adsorbate from the bulk solution to the boundary layer could be a rate
 252 limiting step and this was analyzed using the mass transfer model represented by equation 1.

253
$$\frac{d(\frac{C_t}{C_0})}{dt} = -\beta_L S \text{ ----- (1)}$$

254 where β_L is the external mass transfer coefficient. Fig. 3c represents the plot of mass transfer
 255 model i.e. C_t/C_0 versus t . The external mass transfer coefficient (β_L) was calculated from the slope of
 256 the same plot. The $\beta_L S$ values varied from $2 - 5 \times 10^{-4}$ which were two orders and eight orders of
 257 magnitude lower than the adsorption of Cd onto elemental selenium nanoparticles [16] and the
 258 adsorption of Cu onto dried activated sludge [17]. The lower values shows that the external mass
 259 transfer is not the rate limiting step (Table 2) [16].

260 Film diffusion model or Boyd's kinetic model (Eq. 2) was used to identify whether the
 261 diffusion of adsorbate across the boundary layer was a rate-limiting step.

$$262 \quad \ln \left[\frac{1}{(1-F^2(t))} \right] = \frac{\pi^2 D_e t}{r^2} \text{-----} (2)$$

263 Where $F(t) = q_t/q_e$; D_e is the effective diffusion coefficient (m^2/s); r is the radius of the
 264 spherical adsorbent particle [18]. If the plot of $\ln \left[\frac{1}{(1-F^2(t))} \right]$ vs t is a straight line and passing through
 265 the origin then the film diffusion is the rate limiting step [18]. Previous study [19] reported that the
 266 spherical equivalent diameter of the torrefied biomass sieved to a particle size of of 112 – 125 μm
 267 was 200 μm . According to that, it was assumed that the torrefied biomass particle is spherical with a
 268 particle diameter of 150 μm . The internal diffusion coefficient (D) was calculated from the slope of
 269 the plot presented in Fig. 3d. From the same figure, it can be observed that the plots do not pass
 270 through the origin (intercept of X, Y, Z and t for 25, 50, 100 and 150g/L), showing that the diffusion
 271 of adsorbate across the boundary layer is the rate-limiting step in case of adsorption of furfural on to
 272 the torrefied biomass.

273 The intra-particle diffusion model (Eq. 3) was used to identify the transfer of furfural from
 274 the external surface of the adsorbate to sites through pores of the torrefied biomass.

$$275 \quad q_t = k_{id} t^{1/2} + C \text{-----} (3)$$

276 where q_t is the equilibrium adsorption (mg/g) at time t and k_{id} is the intra-particle diffusion rate
 277 constant. The multi-linear plots (with average $R^2 > 0.97$ for the first and second zone) represents that
 278 the adsorption is controlled by two mechanisms (Figure 3e, Table 2). The first stage of the
 279 intraparticle diffusion model (webber-Morris graph) represents the external mass transfer and the
 280 second stage represents the diffusion [20]. The first linear phase lasted for 2 h while the second linear
 281 phase lasted for another 10 h (Figure 3e). The intercept of the first linear zone is also quite small
 282 (intercept = XX), suggesting that the intraparticle diffusion is the rate-limiting step.

283 The rate-limiting step of intraparticle diffusion was also evaluated by Bangham's kinetic
 284 model represented by equation 4.

$$285 \quad \log \log \left[\frac{C_0}{C_0 - q_t m} \right] = \log \left(\frac{k_b m}{2.303 V} \right) + \alpha \log(t) \text{ ----- (4)}$$

286 where C_0 is the initial concentration of the adsorbate (mg/L), V is the volume of solution (L),
 287 m is the mass of the adsorbent (g/L), and k_b and α are the constants. The linearity of the plot between
 288 $\log \log \left[\frac{C_0}{C_0 - q_t m} \right]$ versus $\log(t)$ represents that pore diffusion is the rate limiting step. The average
 289 $R^2 > 0.96$ was observed for all the dosage experiments. The reasonable linearity of Bangham model
 290 and second zone of intraparticle diffusion model combined with lower β_{LS} values and non-zero
 291 intercept of Boyd's model comsuggest that the furfural diffusion in the pores of torrefied biomass is
 292 the rate limiting step..

293

294 3.4.2 Effect of pH and dosage

295 The influence of pH on the adsorption was studied by varying pH from 2.0 to 9.0 (Fig. 4a).
 296 The q_e (mg of furfural adsorbed per g of torrefied biomass) value did not vary significantly (<10%)
 297 i.e. from 41 (± 4.3) to 37 (± 2.6) when the pH was increased from 2.0 to 9.0, respectively. During
 298 these experiments, the equilibrium pH varied from XX to ZZ. The effect od dosage on furfural

299 adsorption was studied by increasing the dosage from 25 to 150 g/L of torrefied biomass, at 12 h of
 300 residence time. The furfural removal increased from 17 (at 25g/L) to 77% (150g/L) (Fig. 4b). The q_e
 301 values were 41 (± 3.41) and 31 (± 0.61) (mg of furfural adsorbed per g of torrefied biomass) for 25
 302 and 150 g/L dosage, respectively, at 12 h of residence time.

303 <Figure 4>

304

305 3.4.3 Adsorption isotherms

306 The variation of q_e (mg of furfural adsorbed per g of torrefied biomass) with the equilibrium
 307 concentration of furfural (Figure 5a) When the initial concentration was varied from 300 to 6000
 308 mg/L the q_e of furfural onto torrefied biomass was increased from 4.1 (± 0.13) to 36.9 (± 3.2) (mg of
 309 furfural adsorbed per g of torrefied biomass), respectively. The maximum q_e value (i.e. 38 mg of
 310 furfural adsorbed per g of torrefied biomass) was observed at an initial concentration of 5500 mg/L.

311 <Figure 5>

312 The isotherms were modeled using the linearized Langmuir (equation 5) and Freundlich
 313 models (equation 6).

314
$$\frac{C_e}{q_e} = \frac{C_e}{q_m} + \frac{1}{k_L q_m} \text{-----} (5)$$

315 C_e is the equilibrium concentration of the furfural (mg), q_e (mg of furfural adsorbed per g of
 316 torrefied biomass) is the amount of furfural adsorbed at equilibrium (mg/g), q_m is the monolayer
 317 adsorption capacity or the maximum adsorption capacity (mg of furfural adsorbed per g of torrefied
 318 biomass). k_L is the Langmuir constant which represents adsorption energy (L/g).

319
$$\ln q_e = \ln k_f + \left(\frac{1}{n}\right) \ln C_e \text{-----} (6)$$

320 Where k_f is adsorbent capacity ((mg/g) (L/mg)) $^{1/n}$ and n is the intensity of the adsorption.

321 Figure 5b and Figure 5c shows the linear fitting between concentration (q_e) and the
322 equilibrium concentration (c_e) for Langmuir and Freundlich models respectively. The evaluated
323 constants are presented in Table 3. It was observed that both the Freundlich model fitted better with
324 R^2 of 0.98 compared to 0.94 for Langmuir model. The Freundlich constants k_f and n were 0.274
325 (mg/g) (L/g) and 1.654 respectively suggesting favorable adsorption.

326

327 *3.5 Batch adsorption of torrefaction condensate*

328 Figure 6 shows adsorption (%) of different compounds from torrefaction condensate at 250
329 g/L of torrefied biomass dosage. The torrefied biomass adsorbed up to 54% of furfural from the
330 torrefied condensate. Hydroxymethylfurfural (5-HMF), another important inhibitor present in
331 torrefaction condensate, was also adsorbed up to 25%. Around 23% and 60% of furans such as 2(5H)-
332 furanone and 5-methyl-2-furancarboxaldehyde were adsorbed, respectively. In case of phenolic
333 compounds, 74% of coniferyl aldehyde was adsorbed. Around 52, 47 and 56% of other phenolics
334 such as guaiacol, creosol, and vanillin were adsorbed, respectively. In case of organic acids, 21% of
335 formic acid and just 11% of acetic acid was adsorbed. In contrast, concentration of propionic acid
336 was increased by 12%.

337 <Figure 6>

338

339 *3.6 Column adsorption study*

340 *3.6.1 Column adsorption of standard furfural solution*

341 Column adsorption studies of aqueous furfural solution was carried out at two different
342 column diameters i.e. 10 and 20 mm. The furfural uptake and the time required to reach adsorption
343 saturation was increased with increasing column diameter.

344 In case of 10 mm diameter column (Fig. S5a in Supplementary Information) the breakthrough
345 time (i.e. $C/C_0 > 2\%$) was 10 min and the saturation time (i.e. $C/C_0 > 95\%$) was around 80 min. The
346 breakthrough time and saturation time in 20 mm diameter column (Fig. S5b) was around 150 and 380
347 min respectively. This analysis shows that 20 mm diameter column will be more effective for
348 adsorption of inhibitory compounds from torrefaction condensate. Hence, the column with 20 mm
349 diameter and 200 mm bed length was considered for the column adsorption of torrefaction
350 condensate.

351 *3.6.2 Column adsorption of torrefaction condensate*

352 Figure 7 represents the breakthrough curves of different compounds present in torrefaction
353 condensate. The adsorption (%) presented in Fig. 7 were based on the differences in GC-MS peak
354 area of the respective compounds before and after adsorption.

355 <Figure 7>

356 The maximum adsorption of furfural observed was 60% and the saturation time was 50 min.
357 From Fig. 7b, it can be observed that 5-HMF reached saturation within 5 min. The maximum
358 adsorption for other furans such as 5-methyl-2-Furancarboxaldehyde, and 2(5H)-Furanone was 61
359 and 28% and the saturation time was 50 and 30 min, respectively.

360 All the phenolic compounds followed similar adsorption pattern. Similar to the batch
361 experiments, coniferyl aldehyde had highest adsorption of 64%. At the same time, vanillin has the
362 least adsorption (30%). Coniferyl aldehyde has the highest saturation time (90 min) than other
363 compounds reported in this study. The maximum adsorption of other phenolic compounds such as
364 guaiacol, cresol and vanillin was 48, 43 and 30% and the saturation was around 50, 30 and 15 min,
365 respectively.

366 The breakthrough curves of organic acids in torrefaction condensate such as formic, acetic
367 and propionic acids were shown in Fig. 7c. The maximum adsorption of formic acid was around 60%,

368 which was higher than in batch adsorption (20%). Whereas, only around 5% of acetic acid has been
369 adsorbed. The changes in the concentration of acetic acid during time course (between 50-150 min)
370 could be possibly due to a tradeoff between their methyl ester counterparts (as seen in Fig. 7d) and
371 not because of actual adsorption on to the torrefied biomass. Moreover, finally we were able to retain
372 95% of acetic acid in the condensate after 180 min of column adsorption. In case of propionic acid;
373 the column adsorption study followed the batch adsorption by resulting in slight increase in their
374 concentration (~17% after 180 min) possibly due to decrease in water content.

375 The concentrations of other compounds such as 2-propanone, 1-hydroxy- (acetol) and 1-
376 hydroxy-2-butanone were more stable and no adsorption of these compounds was observed. In
377 addition to these two compounds, hydroxy-acetaldehyde was least adsorbed (< 1% at 50 min) by
378 torrefied biomass.

379

380 *3.7 Anaerobic digestion batch assay*

381 The torrefaction condensate, detoxified with 250 g/L of torrefied biomass dosage was used in
382 AD batch assays. Figure 8 shows the cumulative methane yield from AD of torrefaction condensate
383 before and after adsorption at the end of 35 d for 0.1 and 0.2 $VS_{\text{substrate}}:VS_{\text{inoculum}}$ loadings. The
384 respective methane yield (mL/g VS) for torrefaction condensate before and after detoxification was
385 689 and 695 for 0.1 $VS_{\text{substrate}}:VS_{\text{inoculum}}$ and 699 and 487 for 0.2 $VS_{\text{substrate}}:VS_{\text{inoculum}}$.

386 <Figure 8>

387

388 **4. Discussion**

389 *4.1 Effect of adsorption of furfural on to torrefied biomass*

390 This study, for the first time, demonstrated adsorption of furfural from torrefaction condensate
391 using torrefied biomass in order to make torrefaction condensate more suitable and less toxic for

392 microbial bioconversion. About 60% of furfural has been adsorbed from the torrefaction condensate,
393 meaning the reduction in furfural from 9000 to 3600 mg/L at 250 g/L dosage. We have handled very
394 high concentrations of furfural when compared to the studies dealing with biomass hydrolysates,
395 typically in range of 200–3000 mg-furfural/L [5–7,21]. Eventhough we have used high dosage of
396 torrefied biomass as adsorbent, this will not have a negative impact on the overall process considering
397 the fact that the adsorbent is from the same streamline (torrefied biomass pellet production) and
398 following adsorption, they will be mixed back with the rest of the torrefied biomass and taken for
399 regular application. **Moreover, no wastes will be generated out of this process.**

400 Björklund et al. [21] studied the removal of fermentation inhibitors from spruce wood
401 hydrolysate using the lignin as an adsorbent and was able to remove 49% of furfural, 27% of 5-HMF
402 and 36% of phenols at 100 g/L of lignin dosage. These values were close to the ones reported in this
403 study for example, removal of 34% of furfural, 14% of 5-HMF and 33% of phenols with 100 g/L
404 torrefied biomass. These values have been achieved in this study inspite of having the initial
405 concentrations around 10 times higher than the ones reported earlier [21]. Monlau et al. [22] studied
406 the applicability of pyrolysis chars produced from solid anaerobic digestion digestate to remove the
407 inhibitory compounds from Douglas-fir wood hydrolysate. They reported that 99% of furfural and
408 95% of 5-HMF was removed from the hydrolysate at 60 g/L dosage and 24 h contact time where
409 initial concentration of both the compunds was 1000 mg/L suggesting q_e (mg of furfural adsorbed per
410 g of adsorbent) of 16.6 mg/g. This value is lower than the one obtained for torrefied biomass ($36.9 \pm$
411 3.2 mg/g). Further, using torrefied biomass for adsorption of these compounds would have multiple
412 benefits within the refinery. Firstly, removing inhibitory compounds from the condensate will allow
413 them to be utilize for biomethane production. Secondly, increasing moisture content of the biomass
414 and compounds adsorbed onto the biomass would be useful in later stages of refinery in improving
415 the biomass pelletization.

416

417 *4.2. Mechanism of adsorption of furfural on to torrefied biomass*

418 The adsorption of main inhibitory compound furfural on to torrefied biomass is likely due to
419 hydrophobic interaction. The non-effect of pH on the adsorption of furfural points in the direction of
420 hydrophobic interaction (Fig. 5). As the pH varies from 2.0 to 9.0, the deprotonation of the biomass
421 would take place and thus, increasing the number of charged sites. However, the increase in the
422 number of charged sites had no effect on the adsorption of furfural on the torrefied biomass suggesting
423 non-electrostatic mechanisms. Furthermore, adsorption of hydrophobic compounds such as furfural
424 and phenols while non-adsorption of hydrophilic compounds such as acids suggest the adsorption by
425 means of hydrophobic interaction. In addition, the surface of the torrefied biomass is hydrophobic
426 because of the reduced oxygen content [1] further suggesting the hydrophobic interaction between
427 furfural and torrefied biomass. Indeed, the adsorption of furfural from pine needle hydrolysates on to
428 polystyrene-divinylbenzene (XAD-4) copolymers has described as a hydrophobic interaction [23].
429 As the hydrophobic interactions are spontaneous, the adsorption of furfural on to the hydrophobic
430 sites on the torrefied biomass would be quite fast. This is also supported by the good fitting of kinetic
431 data to the pseudo second order kinetics, suggesting that the adsorption mechanism is mainly
432 chemisorption i.e. a fast favorable reaction with negative ΔG (Gibbs Energy).

433 Prior to the adsorption of furfural to the hydrophobic sites in the torrefied biomass, furfural
434 has to reach in close proximity of the sites from the bulk solution. This is done in three steps – arriving
435 of furfural from the bulk solution to the boundary layer, transfer of furfural from the boundary layer
436 to the external surface of torrefied biomass passing through the film or boundary layer and diffusion
437 of furfural to the hydrophobic adsorption site [24]. The reasonable linearity of the second stage
438 intraparticle diffusion model (Fig. 3e) (average $R^2 > 0.97$) and Bangham model (Fig. 3f) (average
439 $R^2 > 0.96$) and the plots not passing through the origin for film diffusion model (Fig. 3d) points out
440 that the furfural passage through micropore diffusion in the torrefied biomass is rate-limiting steps.
441 However, further controlled experiments are required to confirm this finding.

442 The reason for the micropore diffusion to be the rate limiting step can be due to the
443 hydrophobic nature of both furfural and torrefied biomass. As the torrefaction condensate is
444 predominantly made of water (water content > XX%), the furfural molecule, being hydrophobic, will
445 be in cluster. The external surface of the torrefied biomass would have minimized the hydrophobic
446 sites present or only hydrophilic sites would be present. The bulk of the hydrophobic sites would be
447 present more deep in the torrefied biomass. This would result in the need for furfural to diffuse from
448 the external site to internal hydrophobic sites. This is well reflected in diffusion being rate-limiting
449 step in intraparticle diffusion model and Bangham model.

450

451 4.3 Torrefaction temperature effect on to the adsorption property of torrefied biomass

452 At a temperature of 225 °C, a minor portion of hemicellulose is degraded and the volatiles are
453 mainly H₂O and CO₂, which could have caused the low pore distribution on torrefied biomass [26].
454 As the severity of the torrefaction increases (for example at 275 °C) the further degradation of
455 hemicellulose and minor portion of cellulose and lignin occurs, which increases the release of
456 volatiles and there by increases the micro pores. According to Reza et al. [12] and Chen et al. [26], it
457 is because the precipitated tar plugs the existing pores to generate new pores and thereby results in
458 the decreased pore size and increased surface area. However, as the temperature further increases to
459 300 °C, the existing pores are widen and enlarged which results in the decreased surface area (Fig. 1
460 and Table 1). The adsorption of furfural increases with the increasing torrefaction temperature and
461 this could be mainly because of the enlarged pores or increase in number of sites or both. Further, as
462 the severity of the torrefaction increases, the existing pores on the biomass will enlarge and the these
463 enlarged pores allows the furfural solution to diffuse more rapidly into torrefied biomass structures
464 and there by increases the surface contact. . The higher adsorption of furfural by torrefied biomass
465 produced at 300°C with larger pore size and increased diffusion also reflect that the micropore
466 diffusion is involved in adsorption mechanism.

467 *4.4 Anaerobic digestion of torrefaction condensate*

468 The preliminary study on AD of detoxified torrefaction condensate showed that the proposed
469 adsorption process has improved the methane production. As expected, no inhibition was observed at
470 0.1 $VS_{\text{substrate}}:VS_{\text{inoculum}}$ loading and the methane production was similar for both detoxified and
471 original torrefaction condensate for the initial 5 d. However, the methane production with detoxified
472 torrefaction condensate started increasing rapidly after 5 d in comparison with original condensate.
473 After 20 d, methane production saturated for both the setups with around 700 mL/g VS. In case of
474 0.2 $VS_{\text{substrate}}:VS_{\text{inoculum}}$ loading, owing to the inhibitory concentrations of compounds in torrefaction
475 condensate, there was a prolonged lag phase (25 d) for methane production in case of original
476 condensate. Whereas, as a result of adsorption, the detoxified condensate started produced methane
477 just within 15 d, ie. 10 d faster than with the original condensate. At the same time methane production
478 was higher in case of detoxified condensate (699 mL/g VS) than with original condensate (487 mL/g
479 VS) at the end of 35 d. The methane yield from torrefaction condensate reported in this study (700
480 mL/g VS) is comparable with substrates such as used vegetable oil (648 mL/g VS) [27] and co-
481 digestion of 60% of grease trapped sludge with 40% sewage sludge (845 mL/g VS) [28].

482 Eventhough, methane production is better with detoxified condensate, the lag phase for
483 methane production is still longer with with 0.2 $VS_{\text{substrate}}:VS_{\text{inoculum}}$ loading when compared with 0.1
484 $VS_{\text{substrate}}:VS_{\text{inoculum}}$ loading. This could be because of only partial removal of inhibitory compounds
485 from the torrefaction condensate. For example, around 3600 mg/L of furfural was present in the
486 condensate even after adsorption. According to [29], the furfural concentration at 2000 mg/L could
487 inhibit the AD process and increases the lag phase. Further decrease in the furfural concentration
488 could be possibly achieved through a sequential batch/column adsorption. Nevertheless,
489 Doddapaneni et al. [4] reported that microbes could be adapted through cyclic batch AD to decrease
490 the lag phase in methane production. Thus, improving the methane production with little or no lag

491 phase, with higher dosages of torrefaction condensate, is possible and this could be a subject of further
492 investigation.

493

494 4.5 Adsorption scale-up

495 The torrefaction plant capacity proposed by Pirragila et al. [30] i.e. 200 000 ton of torrefied
496 biomass/annum with 8400 operating hours was considered here to understand the flow rate of torrefied
497 biomass in an industrial scale torrefied biomass plant. If it is assumed that 50% of torrefied biomass
498 goes to adsorption process and 50% goes directly to the pelleting section, then 285 ton of torrefied
499 biomass need to be handled at adsorption section per day (24 h). The bulk density of torrefied wood
500 is between 200 – 400 kg/m³ [31]. Considering the bulk density of 300 kg/m³, a total volume of 952
501 m³ is required for column adsorption for everyday operation. Handling such a high amount of biomass
502 in column could be difficult and also may increase the capital, operational and maintenace expenses
503 of the torrefaction unit. At the same time, column experiments result from this study shows that
504 furfural adsorption reached to saturation at 50 min in case of 20 mm internal diameter and 300 mm
505 length column with a flow rate of 1 mL/min. This shows that the saturation time for torrefied biomass
506 for furfural adsorption from torrefaction condensate at an initial concentration of 9000 mg/L is very
507 low. This low saturation time results in frequent loading and unloading of the torrefied biomass in
508 column. As the torrefied biomass pellets are continuously produced, the continuous operation of
509 adsorption and desorption is not suitable for the proposed intrgrated approach (Fig. 1). So, column
510 adsorption for the detoxification of torrefaction condensate may not be suitable to integrate with
511 torrefied biomass pellets production.

512 The experimental results for batch adsorption shows that furfural adsorption is spontaneous
513 for first 2 h of contact time i.e 54 % of furfural removal at an initial concentration of 6000 mg/L. The
514 loading and unloading of the torrefied biomass to the adsorption vessel could be easier and it could

515 be easily integrated with the existing torrefaction unit. At the same time the operational expenses for
516 batch adsorption are lower in comparison with column operation [32]. Thus, the batch adsorption
517 could be more feasible to integrate with torrefaction process in the proposed approach (Fig. 1).
518 However, a maximum of 60% of furfural was adsorbed from torrefaction condensate containing 9000
519 mg furfural/L at 250 g/L of torrefied biomass dosage. Indeed, the increased lag phase in case of 0.2
520 $VS_{\text{substrate}}:VS_{\text{inoculum}}$ loading in anaerobic digestion of detoxified torrefaction condensate shows that
521 torrefaction condensate still inhibits the methane production. Thus, a series of adsorption systems
522 would be required for the complete removal of inhibitory compounds from torrefaction condensate.
523 The size of the torrefaction plant may also show significant influence on the selection between batch
524 and column adsorption. However detailed techno-economic analysis will be required to select
525 between batch and column adsorption processes for the proposed detoxification approach, and this
526 could be a subject of further investigation.

527

528 **5. Conclusion**

529 In this study, for the first time, torrefaction condensate was detoxified using torrefied biomass
530 in order to use them as a substrate for methane production. The removal of furfural and other
531 inhibitory compounds was achieved and better methane production by detoxified torrefaction
532 condensate was demonstrated. The pseudo second order kinetics suggesting a hydrophobic interaction
533 between furfural and torrefied biomass was argued. Intraparticle diffusion model and Bangham model
534 combined with effect of torrefaction temperature on furfural adsorption onto torrefied biomass points
535 to micropore diffusion as a rate limiting step. Further, a continuous column detoxification of
536 torrefaction condensate was operated and a way for process integration of this was discussed .

537

538

539 **Acknowledgement:**

540 The authors gratefully acknowledge the TUT Postdoc funding program. The authors would like to
541 thank Suniti Singh, Marja R.T and Leo Hyvärinen from Tampere University of Technology for
542 providing inoculum for AD tests, helping with GC-MS analyses and SEM images, respectively.

543

544 **References:**

- 545 [1] J. Koppejan, S. Sokhansanj, S. Melin, S. Madrali, Status overview of torrefaction
546 technologies, 2012.
- 547 [2] Hawkins Wright, Global demand for torrefied biomass, (2012).
- 548 [3] S.S. Liaw, C. Frear, W. Lei, S. Zhang, M. Garcia-Perez, Anaerobic digestion of C1-C4 light
549 oxygenated organic compounds derived from the torrefaction of lignocellulosic materials,
550 Fuel Process. Technol. 131 (2015) 150–158. doi:10.1016/j.fuproc.2014.11.012.
- 551 [4] T.R.K.C. Doddapaneni, R. Praveenkumar, H. Tolvanen, M.R.T. Palmroth, J. Konttinen, J.
552 Rintala, Anaerobic batch conversion of pine wood torrefaction condensate., Bioresour.
553 Technol. 225 (2017) 299–307. doi:10.1016/j.biortech.2016.11.073.
- 554 [5] J.R. Weil, B. Dien, R. Bothast, R. Hendrickson, N.S. Mosier, M.R. Ladisch, Removal of
555 fermentation inhibitors formed during pretreatment of biomass by polymeric adsorbents, Ind.
556 Eng. Chem. Res. 41 (2002) 6132–6138. doi:10.1021/ie0201056.
- 557 [6] C. Sambusiti, F. Monlau, N. Antoniou, A. Zabaniotou, A. Barakat, Simultaneous
558 detoxification and bioethanol fermentation of furans-rich synthetic hydrolysate by digestate-
559 based pyrochar, J. Environ. Manage. 183 (2016) 1026–1031.
560 doi:10.1016/j.jenvman.2016.09.062.
- 561 [7] M. Soleimani, L. Tabil, C. Niu, Adsorptive Isotherms and Removal of Microbial Inhibitors in
562 a Bio-Based Hydrolysate for Xylitol Production, Chem. Eng. Commun. 202 (2015) 787–798.
563 doi:10.1080/00986445.2013.867258.
- 564 [8] W.H. Chen, J. Peng, X.T. Bi, A state-of-the-art review of biomass torrefaction, densification
565 and applications, Renew. Sustain. Energy Rev. 44 (2015) 847–866.
566 doi:10.1016/j.rser.2014.12.039.
- 567 [9] B. Ghiasi, L. Kumar, T. Furubayashi, C.J. Lim, X. Bi, C.S. Kim, S. Sokhansanj, Densified
568 biocoal from woodchips: Is it better to do torrefaction before or after densification?, Appl.
569 Energy. 134 (2014) 133–142. doi:10.1016/j.apenergy.2014.07.076.
- 570 [10] J.H. Peng, H.T. Bi, C.J. Lim, S. Sokhansanj, Study on Density , Hardness , and Moisture
571 Uptake of Torrefied Wood 2 Pellets, (2013).
- 572 [11] Q. Hu, J. Shao, H. Yang, D. Yao, X. Wang, H. Chen, Effects of binders on the properties of
573 bio-char pellets, Appl. Energy. 157 (2015) 508–516. doi:10.1016/j.apenergy.2015.05.019.
- 574 [12] M.T. Reza, M.H. Uddin, J.G. Lynam, C.J. Coronella, Engineered pellets from dry torrefied
575 and HTC biochar blends, Biomass and Bioenergy. 63 (2014) 229–238.
576 doi:10.1016/j.biombioe.2014.01.038.
- 577 [13] B. Batidzirai, A.P.R. Mignot, W.B. Schakel, H.M. Junginger, A.P.C. Faaij, Biomass
578 torrefaction technology: Techno-economic status and future prospects, Energy. 62 (2013)
579 196–214. doi:10.1016/j.energy.2013.09.035.
- 580 [14] R.W.R. Zwart, J.R. Pels, Use of torrefaction condensate, (2013).
- 581 [15] J. Kramb, A. Gomez-Barea, N. DeMartini, H. Romar, T.R.K.C. Doddapaneni, J. Konttinen,
582 The effects of calcium and potassium on CO₂ gasification of birch wood in a fluidized bed,
583 Fuel. 196 (2017) 398–407. doi:10.1016/j.fuel.2017.01.101.
- 584 [16] R. Jain, D. Dominic, N. Jordan, E.R. Rene, S. Weiss, E.D. van Hullebusch, R. Hübner,

- 585 P.N.L. Lens, Higher Cd adsorption on biogenic elemental selenium nanoparticles, *Environ.*
586 *Chem. Lett.* 14 (2016) 381–386. doi:10.1007/s10311-016-0560-8.
- 587 [17] H. Benaïssa, M. a Elouchdi, Biosorption of copper (II) ions from synthetic aqueous solutions
588 by drying bed activated sludge., *J. Hazard. Mater.* 194 (2011) 69–78.
589 doi:10.1016/j.jhazmat.2011.07.063.
- 590 [18] S. Suresh, S. Sundaramoorthy, *Green Chemical Engineering: An Introduction to Catalysis,*
591 *Kinetics, and Chemical Processes*, CRC Press, 2014.
- 592 [19] H. Tolvanen, T. Keipi, R. Raiko, A study on raw, torrefied, and steam-exploded wood: Fine
593 grinding, drop-tube reactor combustion tests in N₂/O₂ and CO₂/O₂ atmospheres, particle
594 geometry analysis, and numerical kinetics modeling, *Fuel.* 176 (2016) 153–164.
595 doi:10.1016/j.fuel.2016.02.071.
- 596 [20] W.J. Weber, J.C. Morris, Removal of biologically resistant pollutants from waste waters by
597 adsorption, *Adv. Water Pollut. Res.* 2 (1962) 231–266.
- 598 [21] L. Björklund, S. Larsson, L.J. Jönsson, E. Reimann, N.-O. Nilvebrant, Treatment with lignin
599 residue: a novel method for detoxification of lignocellulose hydrolysates., *Appl. Biochem.*
600 *Biotechnol.* 98–100 (2002) 563–75. doi:10.1385/ABAB:98-100:1-9:563.
- 601 [22] F. Monlau, C. Sambusiti, N. Antoniou, A. Zabaniotou, A. Solhy, A. Barakat, Pyrochars from
602 bioenergy residue as novel bio-adsorbents for lignocellulosic hydrolysate detoxification,
603 *Bioresour. Technol.* 187 (2015) 379–386. doi:10.1016/j.biortech.2015.03.137.
- 604 [23] A.K. Agarwal, R.A. Agarwal, T. Gupta, B.R. Gurjar, *Biofuels: Technology, Challenges and*
605 *Prospects*, Springer Singapore, 2017.
- 606 [24] T. Furusawa, J.M. Smith, Fluid-Particle and Intraparticle Mass Transport Rates in Slurries,
607 *Ind. Eng. Chem. Fundam.* 12 (1973) 197–203. doi:10.1021/i160046a009.
- 608 [25] B.G. Tsyntsarski, B.N. Petrova, T.K. Budinova, N. V. Petrov, D.K. Teodosiev, Removal of
609 phenol from contaminated water by activated carbon, produced from waste coal material,
610 *Bulg. Chem. Commun.* 46 (2014) 353–361.
- 611 [26] Q. Chen, J.S. Zhou, B.J. Liu, Q.F. Mei, Z.Y. Luo, Influence of torrefaction pretreatment on
612 biomass gasification technology, *Chinese Sci. Bull.* 56 (2011) 1449–1456.
613 doi:10.1007/s11434-010-4292-z.
- 614 [27] R.A. Labatut, L.T. Angenent, N.R. Scott, Biochemical methane potential and
615 biodegradability of complex organic substrates, *Bioresour. Technol.* 102 (2011) 2255–2264.
616 doi:10.1016/j.biortech.2010.10.035.
- 617 [28] Å. Davidsson, C. Löfstedt, J. la Cour Jansen, C. Gruvberger, H. Aspegren, Co-digestion of
618 grease trap sludge and sewage sludge, *Waste Manag.* 28 (2008) 986–992.
619 doi:10.1016/j.wasman.2007.03.024.
- 620 [29] S. Pekařová, M. Dvořáčková, P. Stloukal, M. Ingr, J. Šerá, M. Koutny, Quantitation of the
621 Inhibition Effect of Model Compounds Representing Plant Biomass Degradation Products on
622 Methane Production, 12 (2017) 2421–2432.
- 623 [30] A. Pirraglia, R. Gonzalez, D. Saloni, J. Denig, Technical and economic assessment for the
624 production of torrefied ligno-cellulosic biomass pellets in the US, *Energy Convers. Manag.*
625 66 (2013) 153–164. doi:10.1016/j.enconman.2012.09.024.
- 626 [31] W. Stelte, Optimization of product specific processing parameters for the production of fuel
627 pellets from torrefied biomass, *Danish Technol. Inst. Cent. Biomass Biorefinery.* (2014).

- 628 [32] S.C. Lee, S. Park, Removal of furan and phenolic compounds from simulated biomass
629 hydrolysates by batch adsorption and continuous fixed-bed column adsorption methods,
630 *Bioresour. Technol.* 216 (2016) 661–668. doi:10.1016/j.biortech.2016.06.007.

631

632

633

634

635

636

637 **Figure Captions**

638

639 **Figure 1.** A biorefinery process involving detoxification of torrefaction condensate and anaerobic
640 digestion for efficient energy integration within torrefied biomass pellet production.

641

642 **Figure 2.** SEM images of torrefied biomass produced at different temperatures (a - b) 225 °C, (c - d)
643 275 °C, (e - f) 300 °C at different resolution. The red arrows represent pores within the torrefied
644 biomass.

645

646 **Figure 3.** Adsorption kinetics plot for (a) contact time vs adsorption (%), (b) pseudo second-order,
647 (c) mass transfer model, (d) film diffusion model, (e) intra-particle diffusion, and (f) pore diffusion
648 model. The initial concentration of furfural: 6000 mg/L; pH of furfural solution: 3.6; torrefied
649 biomass dosage: 25 – 150 g/L; and contact time: 1 – 12 h.

650

651 **Figure 5.** (a) The influence of pH, (varied from 2 -9), and (b) influence of dosage (varied from 25 –
652 150 g/L) on adsorption of furfural using torrefied biomass. The initial concentration of furfural: 6000
653 mg/L, contact time: 12 h.

654

655 **Figure 6.** Adsorption (%) of different compounds in torrefaction condensate with different torrefied
656 biomass dosage (25 – 250 g/L) during batch experiments. Torrefaction temperature: 300 °C and
657 contact time: 12 h.

658

659 **Figure 7.** Breakthrough curves of column adsorption of torrefaction condensate (a) phenolics, (b)
660 furans, (c) acids, and (d) others organic compounds. Column diameter: 20 mm; bed height: 300
661 mm; flow rate: 1 mL/min.

662

663 **Figure 8.** Cumulative methane yield during AD batch assays with detoxified and original torrefaction
664 condensate at 0.1 and 0.2 $VS_{\text{substrate}}:VS_{\text{inoculum}}$ loading. TC = Torrefaction condensate.

665

666 **Table captions**

667

668 **Table 1.** BET surface analysis of torrefied biomass produced at different torrefaction temperatures.

669

670 **Table 2.** Kinetic parameters. The initial concentration of furfural: 6000 mg/L; pH of standard furfural
671 solution: 3.6; torrefied biomass dosage: 25 – 150 g/L; contact time: 1 – 12 h.

672

673 **Table 3.** Isotherm model constants. The initial concentration of furfural (C_0): 300 - 6000 mg/L;
674 contact time :12 h; torrefied biomass dosage: 50 g/L.

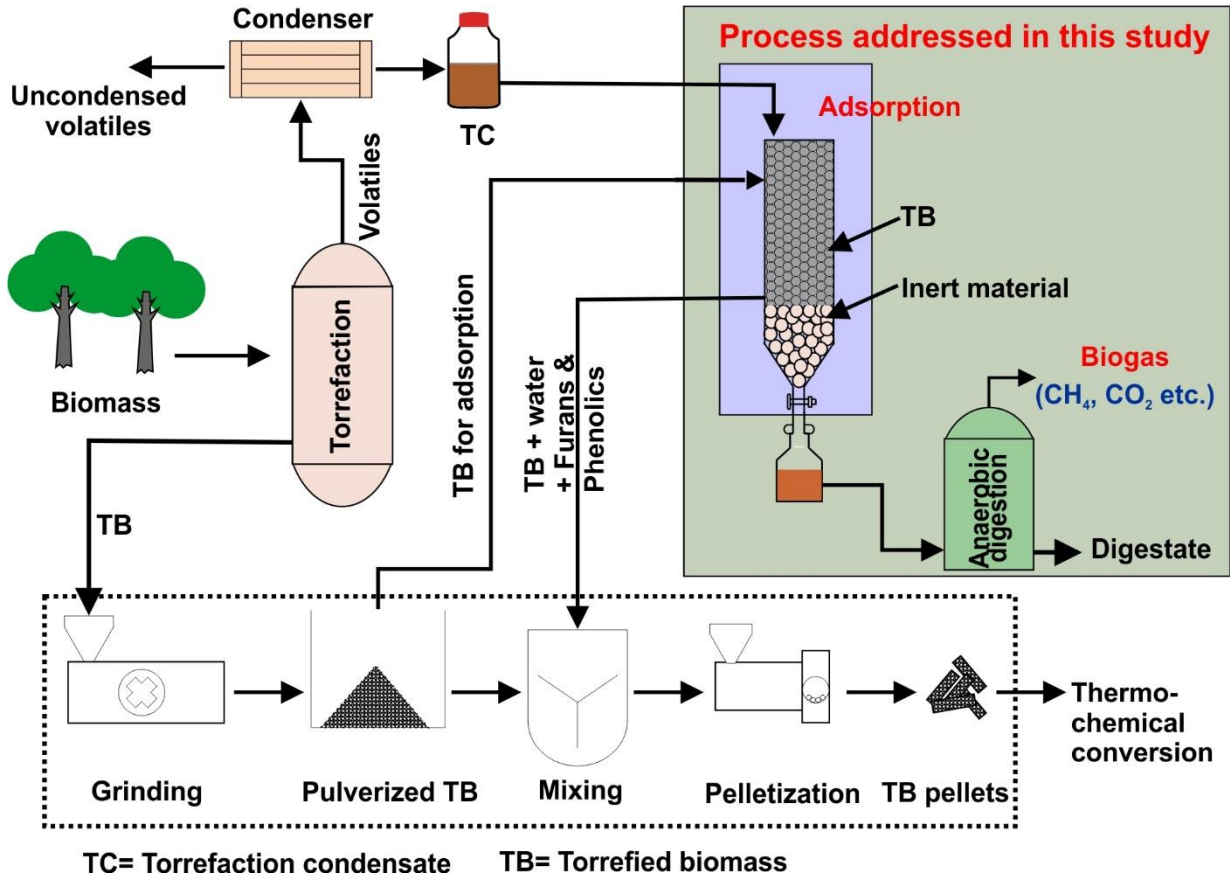
675

676

677 **Figures**

678

679 **Fig. 1**



680

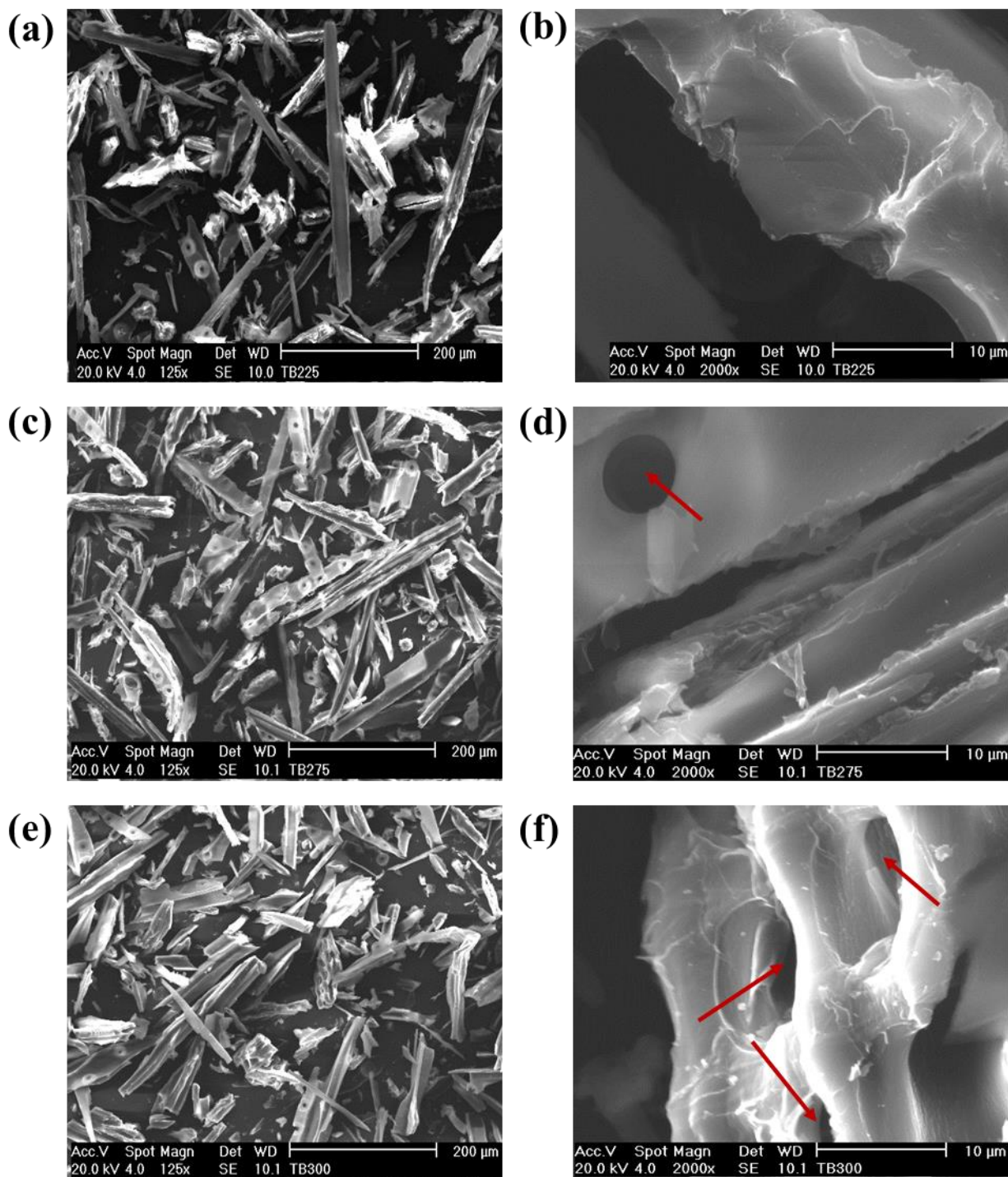
681

682

683

684

685 **Fig. 2**



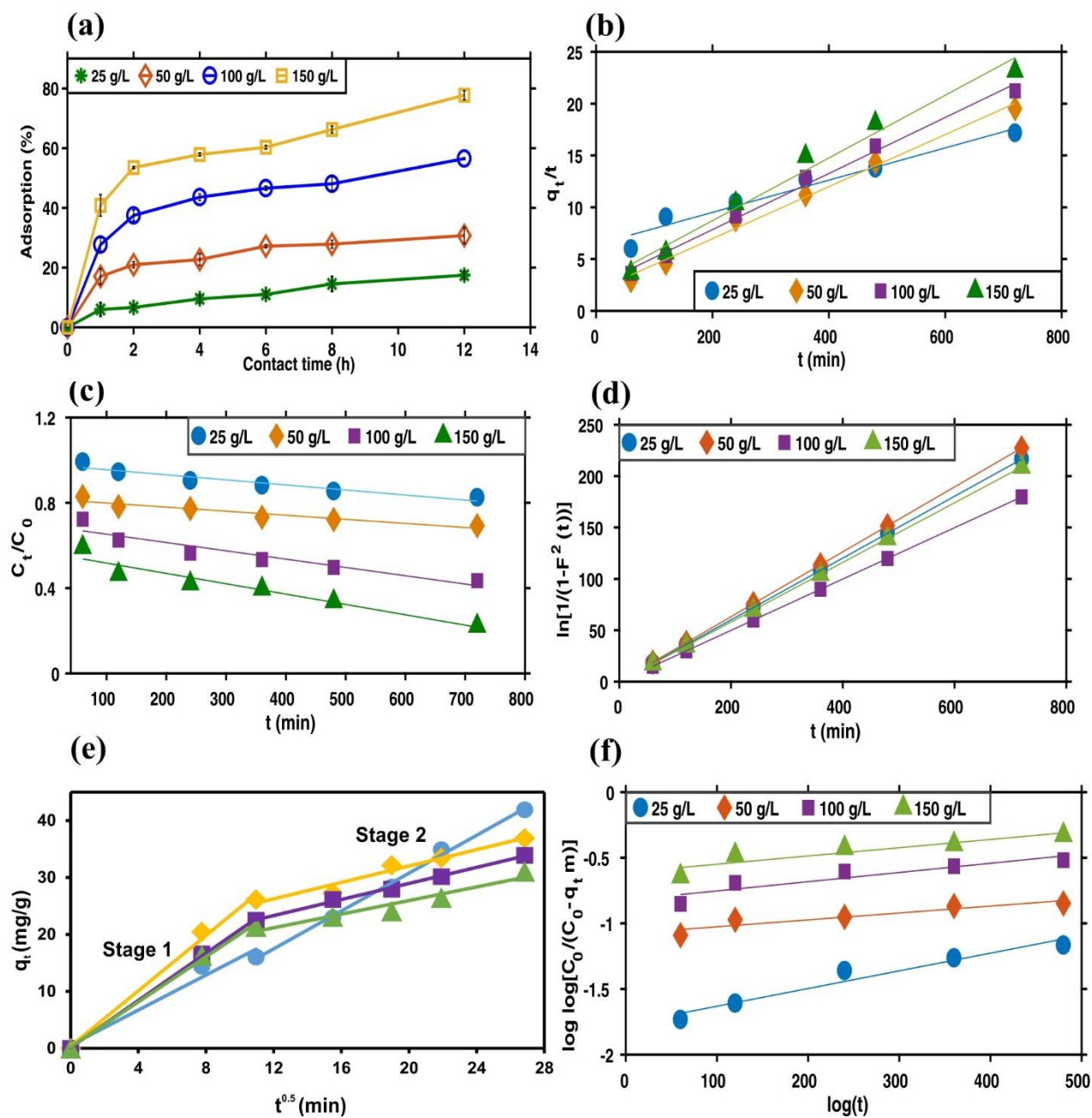
686

687

688

689

690 **Fig. 3**



691

692

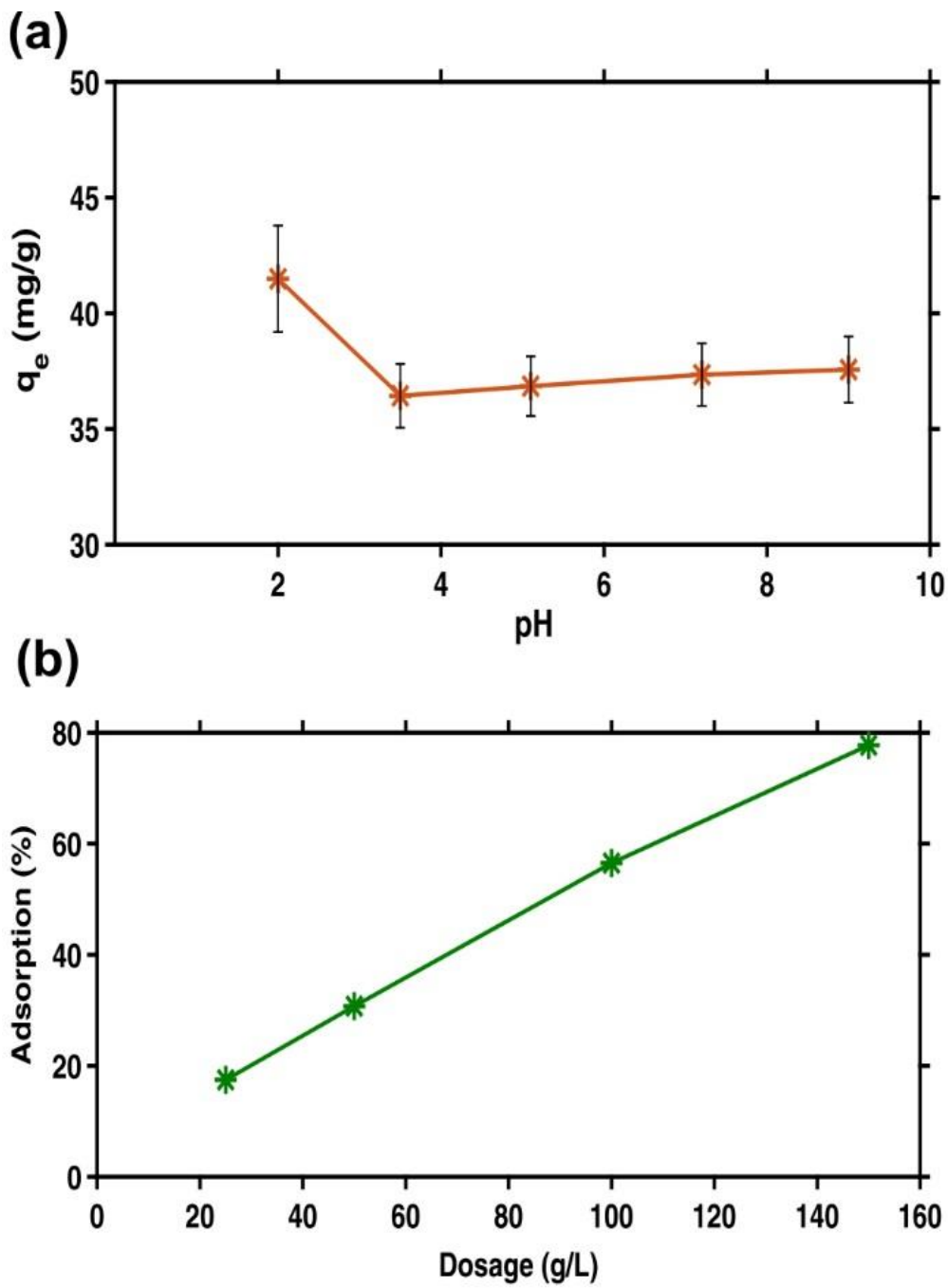
693

694

695

696

697 Fig. 5



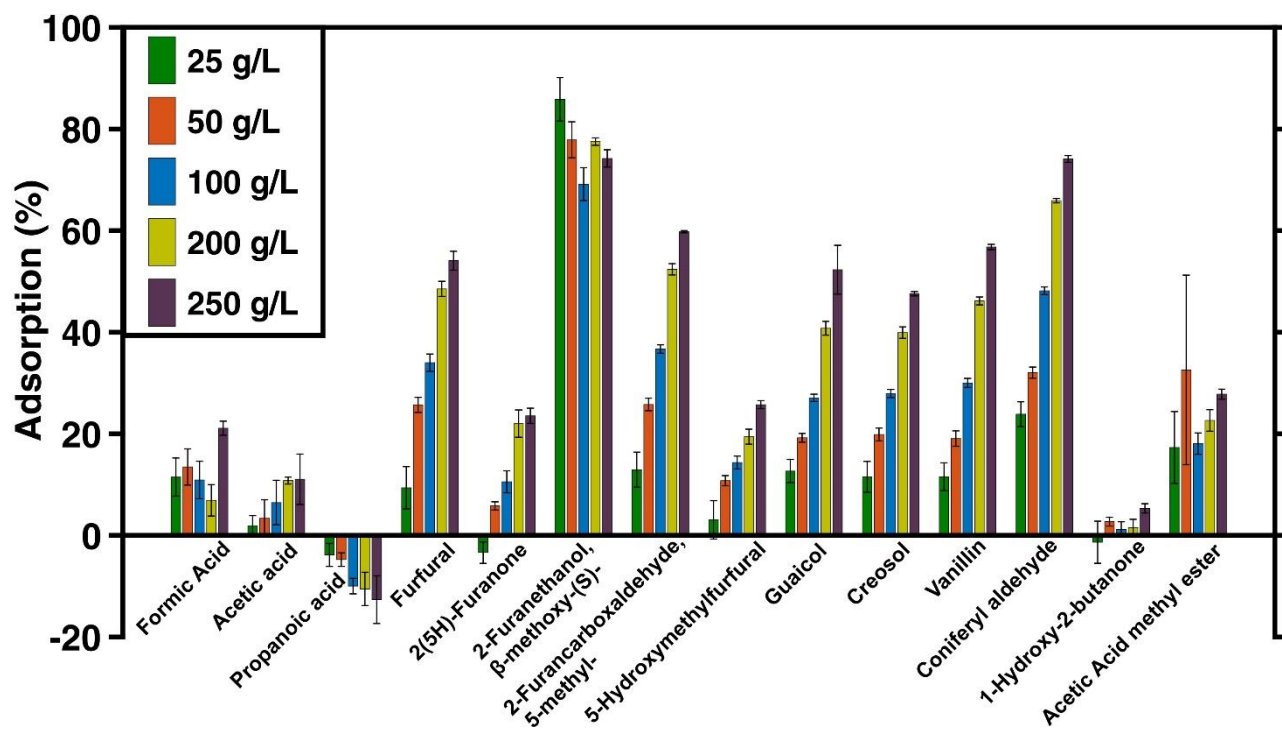
698

699

700

701

702 **Fig. 6**



703

704

705

706

707

708

709

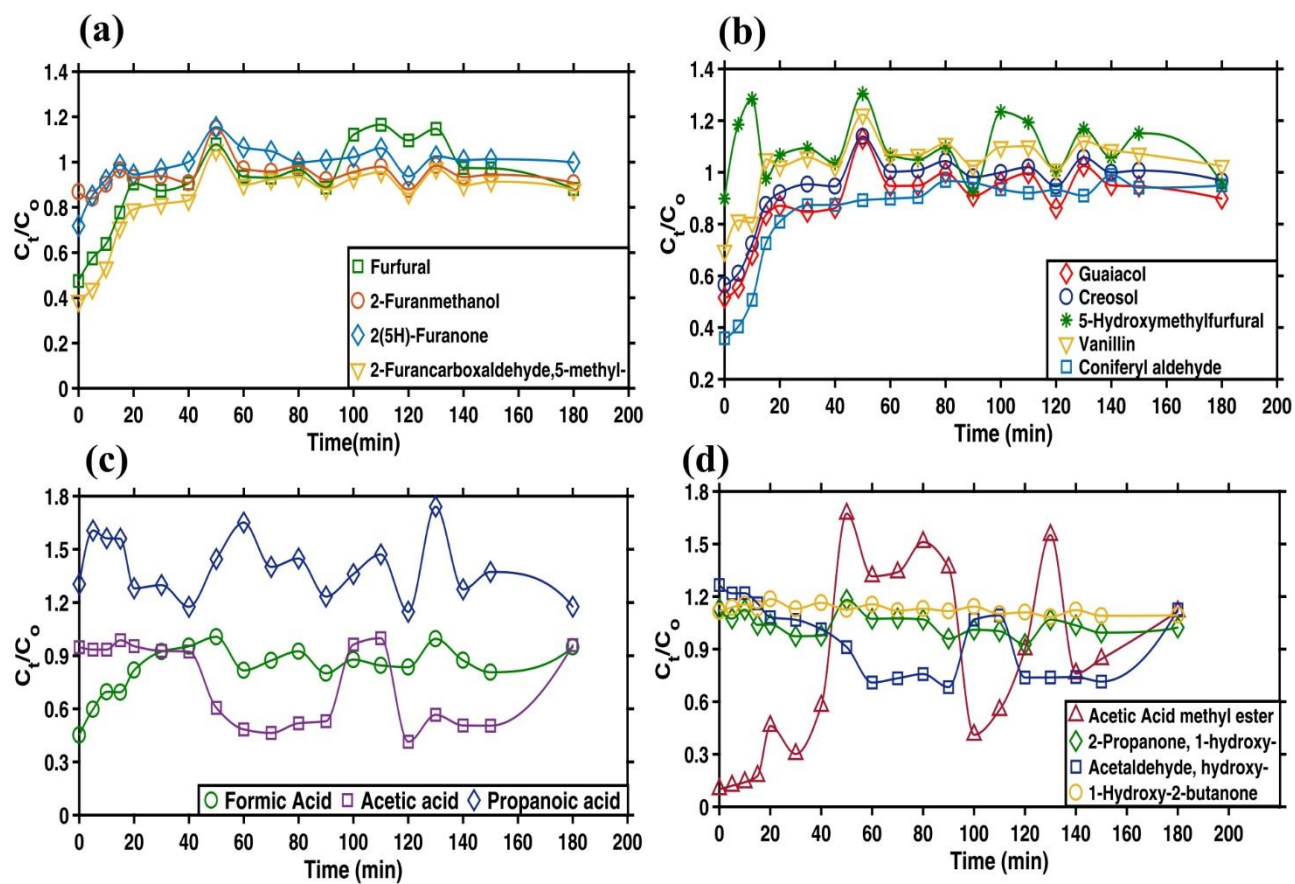
710

711

712

713

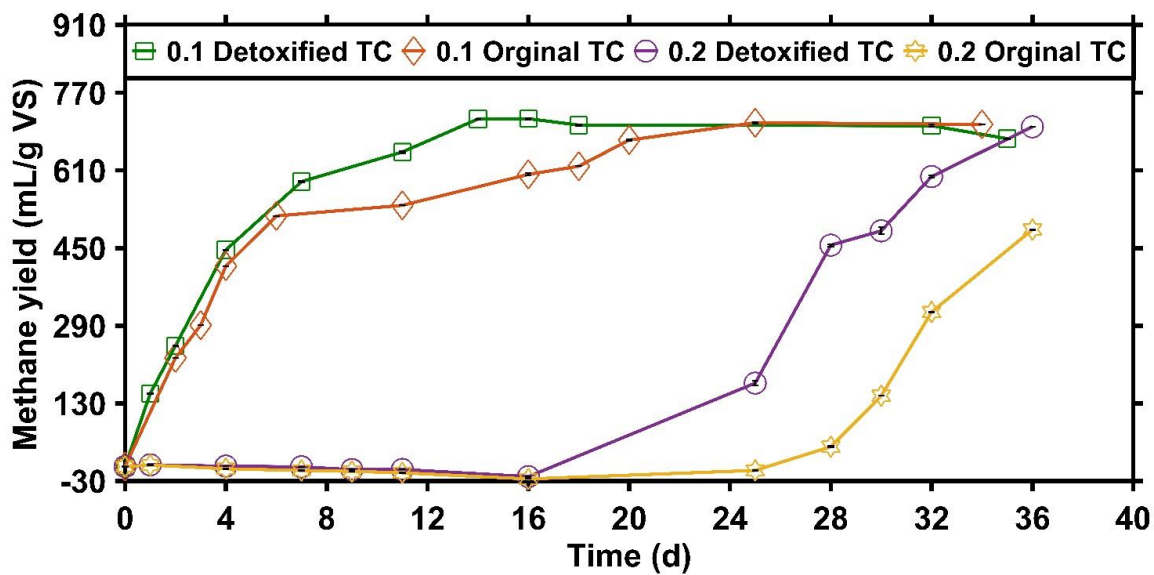
714 **Fig. 7**



715

716

717 Fig. 8



718

719

720

721

722

723

724

725

726

727

728

729 **Tables**

730

731 **Table 1**

Sample	Specific surface area (m ² /g)	Pore Volume (cm ³ /g)	Mean pore diameter (nm)
TB225	Nd	No pores	–
TB275	1.47	0.0065	17.8
TB300	1.10	0.0043	15.7

732

733

734

735

736

737

738

739

740

741

742

743

744

745

746

747

748 **Table 2**

<u>Pseudo first-order model</u>				
Dosage (g/L)	k_f	q_e Cal	R^2	Error %
25	0.00322	37.14	0.9523	0.11
50	0.00368	19.32	0.9593	0.47
100	0.00345	18.95	0.9764	0.44
150	0.00230	14.98	0.929	0.52
<u>Pseudo Second-order model</u>				
Dosage (g/L)	k_s	q_e Cal.	R^2	Error %
25	0.0183	54.64	0.933	0.303
50	0.0251	39.84	0.992	0.07
100	0.0271	36.90	0.993	0.08
150	0.0303	33.00	0.979	0.06
<u>Mass transfer model</u>				
Dosage (g/L)	β_{LS}	R^2		
25	0.0002	0.986		
50	0.0002	0.905		
100	0.0004	0.8927		
150	0.0005	0.9254		
<u>Film diffusion model (Boyd)</u>				
Dosage (g/L)	D_e (m^2/min)	R^2		
25	1.01E-014	0.9195		
50	1.34E-14	0.9597		
100	1.22E-14	0.9846		
150	8.41E-15	0.939		
<u>Intra particle diffusion model</u>				
Dosage (g/L)	k_{id1}	R^2	k_{id2}	R^2
25	1.537	0.9621	1.612	0.9939
50	2.431	0.9934	0.721	0.957
100	2.068	0.9988	0.706	0.9964
150	1.982	0.9963	0.598	0.9345
<u>Pore diffusion model (Bangham's)</u>				
Dosage (g/L)	α	K_{0B}	R^2	
25	0.478	3.13E-04	0.9647	
50	0.259	1.33E-03	0.967	
100	0.356	7.92E-04	0.982	
150	0.368	7.93E-04	0.932	

750 **Table 3**

Langmuir			Freundlich		
q_m (mg/g)	KL (L/mg)	R^2	n	K_f ((g/g) (L/g) ^{1/n})	R^2
55	0.000679	0.9476	1.657	0.174	0.9886

751

752